AD-A130 922 KINETIC STUDIES OF THE REACTIONS OF CH3O2 WITH NO2 AND OH WITH HNO3..(U) GEORGIA INST OF TECH ATLANTA ENGINEERING EXPERIMENT STATION A R RAVISHANKARA ET AL. 1/1

UNCLASSIFIED MAR 83 FAA/EE-83-04 DOT-FA78WA-4259 F/G 4/1 NL

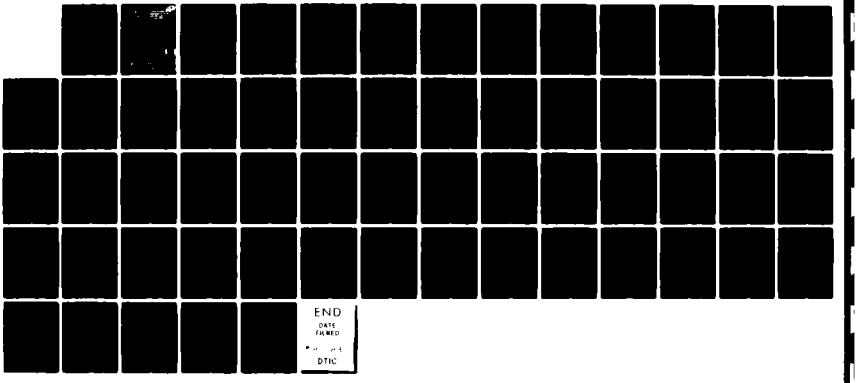

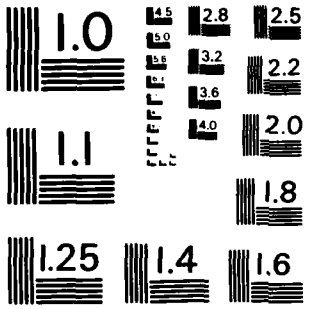

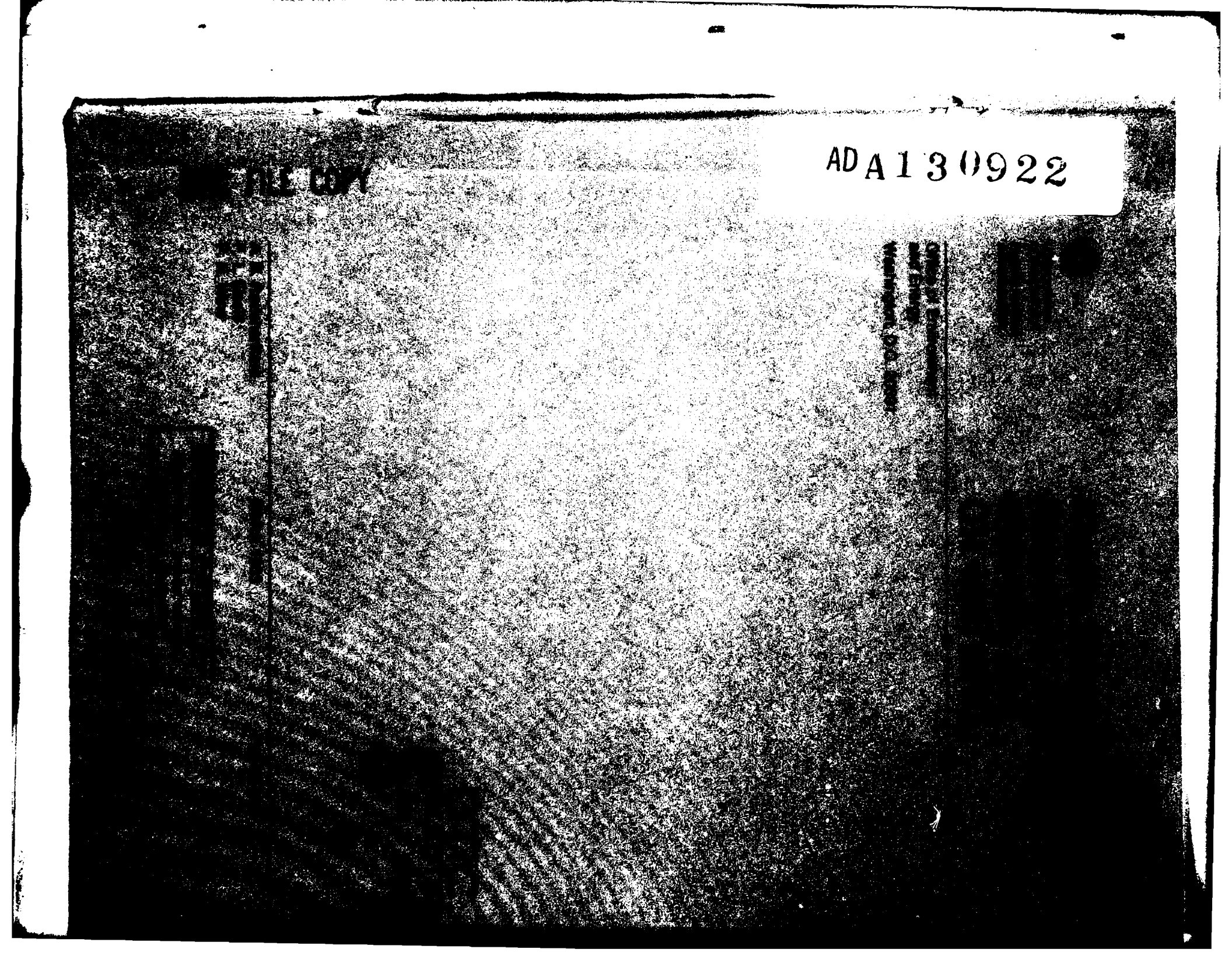
AD A130922

Technical Report Documentation Page

1. Report No.	2. Government Accession No.	3. Recipient's Catalog No.
FAA-EE-83-04	AD-A130922	

4. Title and Subtitle	5. Report Date
KINETIC STUDIES OF THE REACTIONS OF CH_3O_2 WITH NO_2 AND OH WITH HNO_3	March 1983
	6. Performing Organization Code
	8. Performing Organization Report No.
7. Author's	
A.R. Ravishankara, F.L. Eisele and P.H. Wine	
9. Performing Organization Name and Address	10. Work Unit No. (TRAIS)
Georgia Institute of Technology Engineering Experiment Station Atlanta, Georgia 30332	11. Contract or Grant No. DOT-FA-78WA-4259
	13. Type of Report and Period Covered Final Technical Report
12. Sponsoring Agency Name and Address U.S. Department of Transportation Federal Aviation Administration, Office of Environment and Energy, Air Quality Division Washington, D.C. 20591	14. Sponsoring Agency Code
15. Supplementary Notes	

16. Abstract

The technique of Pulsed Laser Photolysis - long path laser absorption is employed to study the kinetics of the reaction $CH_3O_2 + NO_2 \xrightarrow{k_1} CH_3O_2NO_2 + N_2$ and the reaction $OH + HNO_3 \xrightarrow{k_2} NO_3 + H_2O$. The first reaction was measured over the temperature range 253-353K by following the reactant CH_3O_2, while the second reaction was investigated at 298 and 251K by monitoring the product NO_3. At all temperatures, k_1 is found to monotonically increase with increasing N_2 pressure over the range 76-722 Torr, indicating that reaction occurs predominantly by addition. The dependence of k_1 on N_2 pressure shows that the reaction is in the fall-off region between second and third order kinetics. These results are compared with previous results and their atmospheric implications are discussed. The value of k_2 obtained agrees well with our previous measurements (Wine, et al., J.G.R., 86, 1105, 1981). In addition, the yield of NO_3 in reaction (2) was directly measured to be near unity at both 298 and 251K. Chapters (1) and (2) describe the studies of k_1 and k_2, respectively.

17. Key Words	18. Distribution Statement
Reaction rate coefficients Stratospheric chemistry Tropospheric chemistry Reaction kinetics	This document is available to the public through the National Technical Information Service, Springfield, Virginia 22161

19. Security Classif. (of this report)	20. Security Classif. (of this page)	21. No. of Pages	22. Price
UNCLASSIFIED	UNCLASSIFIED	58	

Form DOT F 1700.7 (8-72) Reproduction of completed page authorized

Abstract

The technique of Pulsed Laser Photolysis - long path laser absorption is employed to study the kinetics of the reaction $CH_3O_2 + NO_2 \xrightarrow{k_1} CH_3O_2NO_2 + N_2$ and the reaction $OH + HNO_3 \xrightarrow{k_2} NO_3 + H_2O$. The first reaction was measured over the temperature range 253-353K by following the reactant CH_3O_2, while the second reaction was investigated at 298 and 251K by monitoring the product NO_3. At all temperatures, k_1 is found to monotonically increase with increasing N_2 pressure over the range 76-722 Torr, indicating that reaction occurs predominantly by addition. The dependence of k_1 on N_2 pressure shows that the reaction is in the fall-off region between second and third order kinetics. These results are compared with previous results and their atmospheric implications are discussed. The value of k_2 obtained agrees well with ~~our~~ previous measurements, (~~Wine, et al., J.G.R., 86, 1105~~, 1981). In addition, the yield of NO_3 in reaction (2) was directly measured to be near unity at both 298 and 251K. ~~Chapters~~ (1) and (2) describe the studies of k_1 and k_2, respectively.

Table of Contents

Introduction

The methylperoxy radical is an important intermediate in reaction sequences through which hydrocarbons are oxidized in both atmospheric and combustion processes. In combustion systems the fate of peroxy radicals is predominantly governed by their reactions with other radicals, while in the atmosphere, and particularly in the polluted troposphere, it is expected that reactions with stable molecules will be important. The major species which can react with CH_3O_2 in the atmosphere include HO_2, NO, NO_2, SO_2, and O_3. The rate constant for the reaction of CH_3O_2 with NO has been recently measured using direct kinetic techniques[1-3] and found to be nearly as fast as the reaction of HO_2 with NO.[4,5] Therefore, in a polluted atmosphere where NO_x concentrations are high, methyl peroxy radicals are expected to react mostly with NO_x species. For the subject reaction of the present investigation,

$$CH_3O_2 + NO_2 + N_2 \xrightarrow{k_1} CH_3O_2NO_2 + N_2 \qquad (1)$$

to effectively compete with the reaction of CH_3O_2 with NO,

$$CH_3O_2 + NO \xrightarrow{k_2} CH_3O + NO_2 \qquad (2)$$

the value of k_1 should be of similar magnitude as that of k_2. If Reaction (1) were a significant path for CH_3O_2 removal, NO_2 production (and the subsequent O_3 generation) would be reduced.

Until recently most rate coefficients for CH_3O_2 radical reactions were obtained by steady state competitive experiments.[6-8] In the past few years direct measurement techniques such as discharge flow-mass spectrometry, flash photolysis-ultraviolet absorption, and molecular

modulation-UV absorption spectroscopy have been adopted for CH_3O_2 radical studies.

To date three direct measurements of k_1 have been carried out. Cox and Tyndall[9] utilized the molecular modulation-UV absorption technique and obtained a value of k_1 which was essentially independent of bath gas pressure. The flash photolysis-UV absorption method has been employed by Adachi and Basco,[10] and Sander and Watson[2] to measure k_1. Adachi and Basco's results are in agreement with those of Cox and Tyndall. However, unlike the previous two measurements, Sander and Watson found Reaction (1) to be pressure dependent. These investigators carried out their experiments under secondary reaction free conditions using a very sensitive probe for CH_3O_2 radicals. Hence, their results appear to be more reliable. There are no previous measurements of k_1 as a function of temperature.

In the present study, k_1 was measured as a function of N_2 diluent gas pressure and temperature using the recently developed technique of pulsed laser photolysis-long path laser absorption. Due to the monochrmoaticity of the photolysis laser, and the resultant photolysis specificity, all unwanted photofragments were essentially eliminated, while the high intensity of the CW 257 nm probing laser beam enabled measurement of very low concentrations of CH_3O_2. Under these secondary reaction free conditions, our measured value of k_1 was found to be pressure dependent in excellent agreement with Sander and Watson. Also, as to be expected for an addition reaction, k_1 was found to increase with decreasing temperature.

The technique of pulsed laser photolysis-laser induced fluorescence was originally proposed to be employed in the study of Reaction (1). CH_3O_2 radicals were to be produced using either 355 nm photolysis of $Cl_2/CH_4/O_2$ mixtures or UV photolysis of azomethane. To follow the course of the reaction either NO_2 reactant in excess CH_3O_2 or CH_2O product in excess NO_2 were to be monitored using laser induced fluorescence.

There were two developments which excluded carrying out laser induced fluorescence detection of CH_2O to map out the course of Reaction (1): a) we could not obtain the expected 10 mW of UV laser output in the intracavity Ar^+ laser pumped tunable dye laser (in fact, we succeeded in obtaining only 20 μW!), and b) in some recent studies it was shown that Reaction (1) proceeds predominantly through an addition mechanism; therefore, the CH_2O product yield is very low, and an unrealistically high detection sensitivity for CH_2O would be needed. For these reasons, we abandoned the idea of monitoring CH_2O.

The second approach of following the NO_2 decay in excess CH_3O_2 was pursued when the first approach failed. The primary requirement for this experiment was the creation of a uniform known concentration of CH_3O_2 by laser photolysis. We have succeeded in obtaining a spatially uniform, 'top hat' profiled laser beam using a segmented aperture optical integrator. With this added capability, we can produce CH_3O_2 radicals in excess over NO_2. Our capability to detect NO_2 via laser induced fluorescence (pumped by the 488 nm output of an argon ion laser) is well developed and has been used in the study of the reaction of CH_3O_2 with NO.[3] However, when we tried to monitor NO_2 in excess CH_3O_2, we found the decay of NO_2 to be non-exponential. The decay rates decreased with time due to the disproportionation reaction,

$$CH_3O_2 + CH_3O_2 \longrightarrow \text{Products} \quad . \qquad (a)$$

The rate coefficient for Reaction (a) is reasonably well known.[2] A simple calculation shows that unless Reaction (1) is very fast, i.e., is $\sim 1 \times 10^{-11}$ $cm^3 molecule^{-1} s^{-1}$, the CH_3O_2 concentration would decrease by more than 10% by the time the NO_2 concentration dropped to 1/e times its original value. Therefore, it was evident that even though we could measure k_1 at low temperatures and high pressures the required range of pressures and temperatures could not be covered.

Upon realizing that our originally proposed methods would be either inapplicable or of limited use, we decided to develop the laser photolysis-long path laser absorption technique. This effort was very successful and we completed the measurement of k_1 as a function of temperature and pressure, as discussed below.

PULSED LASER PHOTOLYSIS-LONG PATH LASER ABSORPTION KINETICS STUDY OF THE REACTION OF METHYLPEROXY RADICALS WITH NO_2

Experimental

A schematic diagram of the apparatus used to study Reaction (1) is shown in Figure 1. A jacketed reactor with an internal volume of ~ 1ℓ and a length of 107 cm was constructed out of pyrex. The cell was maintained at a constant temperature by circulating either methanol (253-298 K) or ethylene glycol (298-353 K) from a temperature controlled circulator through the outer jacket. It was found that the temperature was uniform to within 2°C throughout the length of the cell. On both ends of the reactor two 1/8" thick, 2" diameter quartz (Suprasil 1) plates were attached using O-ring seals and metal clamps. The reactants were premixed in a mixing chamber and slowly flowed through the reactor. At the outlet of the reactor, the pressure in the system was measured using an absolute one-turn Bourdon gauge (Wallace and Tiernan Model FA160-NN) before the gas mixture was pumped out.

Azomethane/N_2 and NO_2/N_2 mixtures were prepared in 12ℓ bulbs on a gas handling system. The bulbs were connected to the mixing chamber using teflon tubing and stainless steel ultra-torr fittings. The rates of flow of the azomethane/N_2 mixture, NO_2/N_2 mixture, N_2, and O_2 into the mixing chamber were controlled by stainless steel needle valves and measured by calibrated mass flow transducers. The tubes leading into the mixing chamber had radial outlets to turbulently mix the gases. The concentration of each component in the reaction mixture was determined from measurements of appropriate mass flow rates and the total pressure. The concentration of NO_2 in the NO_2/diluent mixture was checked (before and after each set of experiments) by simultaneous measurements of the total pressure (of the mixture) and NO_2 absorption

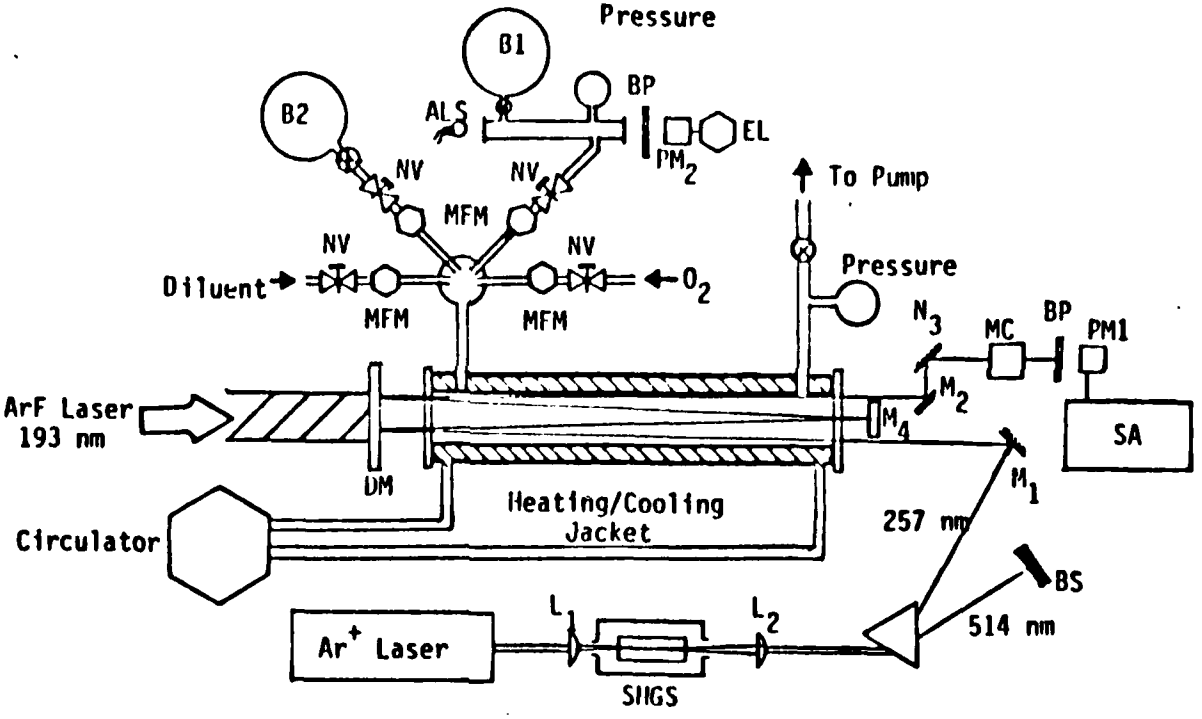

Figure 1. A Schematic Diagram of Pulsed Laser Photolysis-Long Path Laser Absorption Apparatus.

at 366 nm. The measurements were carried out using an Hg pen-ray lamp as the light source, a 70 cm absorption cell, and a bandpass filter-photomultiplier detector combination. The absorption cross section used to determine $[NO_2]$, 5.75×10^{-19} cm^2,[11] has been previously measured in our laboratory and agrees well with the literature value.[12] The azomethane concentration was occasionally checked by a method identical to that for NO_2; the absorption cross section of azomethane was measured to be 1.13×10^{-20} cm^2 at 366 nm, which is slightly higher than the published value,[13] but in agreement with other recent measurements.[14]

Azomethane was prepared as described in Appendix I. NO_2, obtained from Matheson Gas Products, had a stated purity of 99.5%, and was purified by mixing it with UHP O_2 to convert all NO to NO_2, and subsequently subjecting it to freeze-pump-thaw cycles to remove O_2. NO_2 and O_2 were Matheson grade and had stated purity levels of 99.9995% and 99.99%, respectively; these gases were used as supplied.

An ArF excimer laser, the photolysis light source, was housed in an adjoining room, approximately 2 meters from the front window of the reactor. We found this spatial separation to be essential if a uniform beam was to be obtained. (Operation of the laser under slightly fluorine-rich conditions also helped to make the beam more diffuse.) The beam was approximately 2 cm x 7 cm by the time it reached the reactor. The laser beam was transmitted through a custom made dielectric mirror, DM and traveled through the reactor impinging on the MgF_2 coated aluminum mirror M_4 where a fraction of the beam was reflected back into the reactor. Both mirrors DM and M_4 were mounted on precision mirror mounts with vernier control to enable very fine adjustments. (DM was specially coated for us by Acton Research Corp. to have $\sim$ 85% transmisstion at 193 nm and $\geq$ 95% reflectivity at 257 nm.)

The doubled CW 257 nm UV beam was generated as described in Appendix II. This beam was diverted into the reactor using mirror M_1 so as to traverse the volume photolyzed by the ArF laser beam. By adjusting Mirrors DM and M_4, the CW UV beam was multipassed 8 times through the reactor to obtain a path length of $\sim$ 860 cm. The 8th pass was diverted away from the reactor by a small aluminum mirror M_2, passed through a methanol cell and a 257 nm bandpass filter, and detected by a quartz envelope 1P28 (RCA) photomultiplier tube. (It was necessary to use a methanol filter to prevent the 193 nm laser pulse from being detected by the PM tube.) The output of the PM tube was amplified and stored in a signal averager (Tracor-Northern 1500) operating in the analog mode and triggered 150 μsec after the photolysis pulse. (We could not obtain a usable signal in the first 150 μsec due to interference from fluorescence induced by the 193 nm beam.) The PM tube was operated at $\sim$ 600 V to have a resistor bridge current of $\sim$ 1 mA. The anode current was always kept below 1 μA by using suitable neutral density filters to reduce the intensity of the 257 nm beam. To increase the signal-to-noise ratio of the decay curves, 16 to 64 flashes were averaged. The pulse rate of the photolysis laser (0.03 to 0.01 Hz) was such that the contents of the reactor was replaced between consecutive photolysis pulses. This was necessary in order to sweep out the products (which also absorb the probing beam) and use identical gas mixtures for each flash. In preliminary experiments it was established that as long as the cell was swept out between flashes either the laser repetition rate or the flow rate of the mixture through the reactor did not affect the measured value of k_1. The intensity of the transmitted 257 nm beam before photolysis was higher than that obtained when all CH_3O_2 had reacted. This residual absorption has been observed by both Cox and

Tyndall,[9] and Sander and Watson,[2] and is attributed to the absorption by $CH_3O_2NO_2$, the product of Reaction (1). Sander and Watson[2] have shown that the absorption of the analyzing beam by a reaction product which is stoichiometrically coupled to the monitored reactant species by a single reaction (as it is in the present case) does not affect the kientic data that is obtained. In addition, they point out that the proper I_0 value that should be used in the data analysis is the intensity of the 257 nm beam when all CH_3O_2 has reacted, and not the value obtained when $CH_3O_2NO_2$ is absent. It is worth noting that since the intensity of the probing beam was high, the signal-to-noise was excellent and we could easily work with less than 3% initial absorption and still follow the decay of CH_3O_2 down to $\sim$ 4 1/e times!

Results

Reaction (1) was studied as a function of the pressure of the bath gas N_2 and temperature (at 298K, 76-722 torr; at 353K, 330-696 torr; at 253K, 109-510 torr). As pointed out earlier, all experiments were carried under pseudo-first order conditions with $[NO_2] > [CH_3O_2]$. Figure 2 shows typical decays of $[CH_3O_2]$ as a function of time; the decays are exponential and thus confirm the presence of pseudo-first order conditions. The decay of $[CH_3O_2]$ was usually followed, for 3 1/e times. The pseudo-first order rate constant, k_1' ($\equiv$ slope of $\ell n[CH_3O_2]$ vs. t plots) was measured for various values of $[NO_2]$ at each temperature and N_2 pressure. k_1' was then plotted against $[NO_2]$; the slope of this line gave k_1. Figure 3 shows one such plot. It should be pointed out that the fitting procedure we employed (a linear least squares analysis) did not force the k_1' vs. $[NO_2]$ line to a zero intercept; in our system, it is possible to have a non-zero intercept since the entire volume of the reactor was not subjected to the photolysis. The intercepts in all our experiments were small relative to the measured k_1' values.

Table I lists the individual values of k_1' along with all the pertinent experimental conditions. The quoted errors for k_1, calculated from the slope of k_1' vs. $[NO_2]$ plots, are 2σ and reflect the precision of the measurement. The absolute accuracy of the measured values of k_1, is expected to be $\sim$ 20% which includes the error in the $[NO_2]$ measurement.

Table II lists the values of k_1 obtained at various N_2 pressures and temperatures. Figure 4 shows a plot of k_1 as a function N_2 number density at three different temperatures. The solid lines drawn through these points are visual best fits.

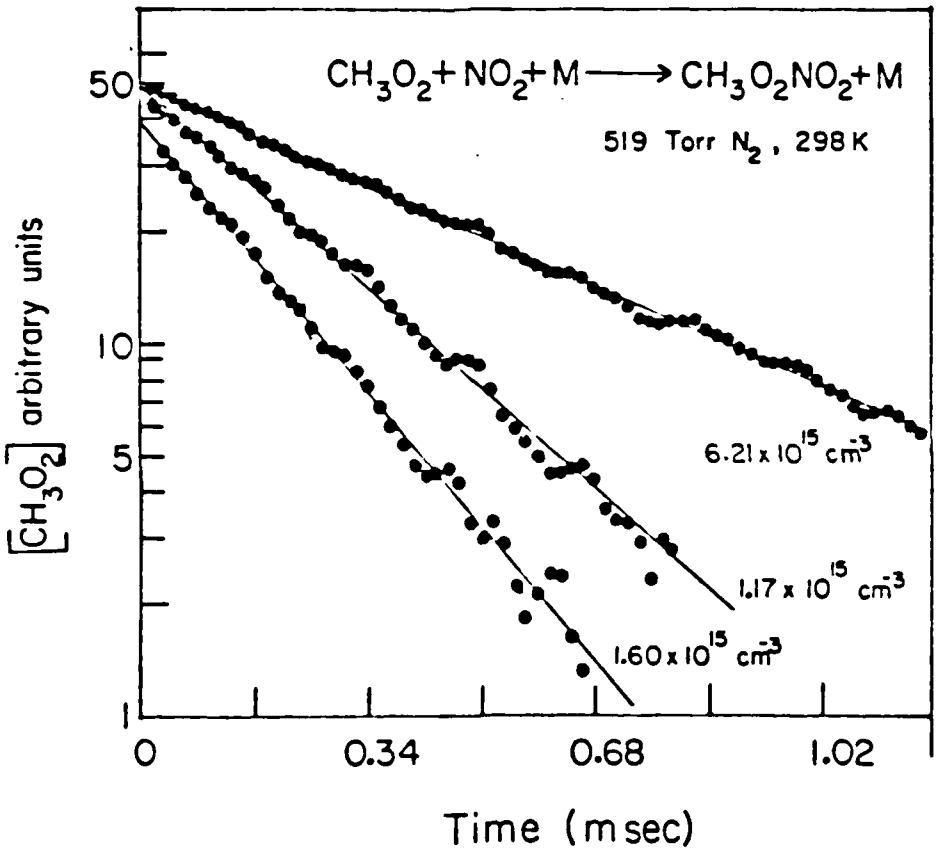

Figure 2. $[CH_3O_2]$ Temporal Profiles in the Presence of Varying Amounts of NO_2. The concentration of NO_2 for each decay curve is shown next to the least squares lines drawn through the experimental points.

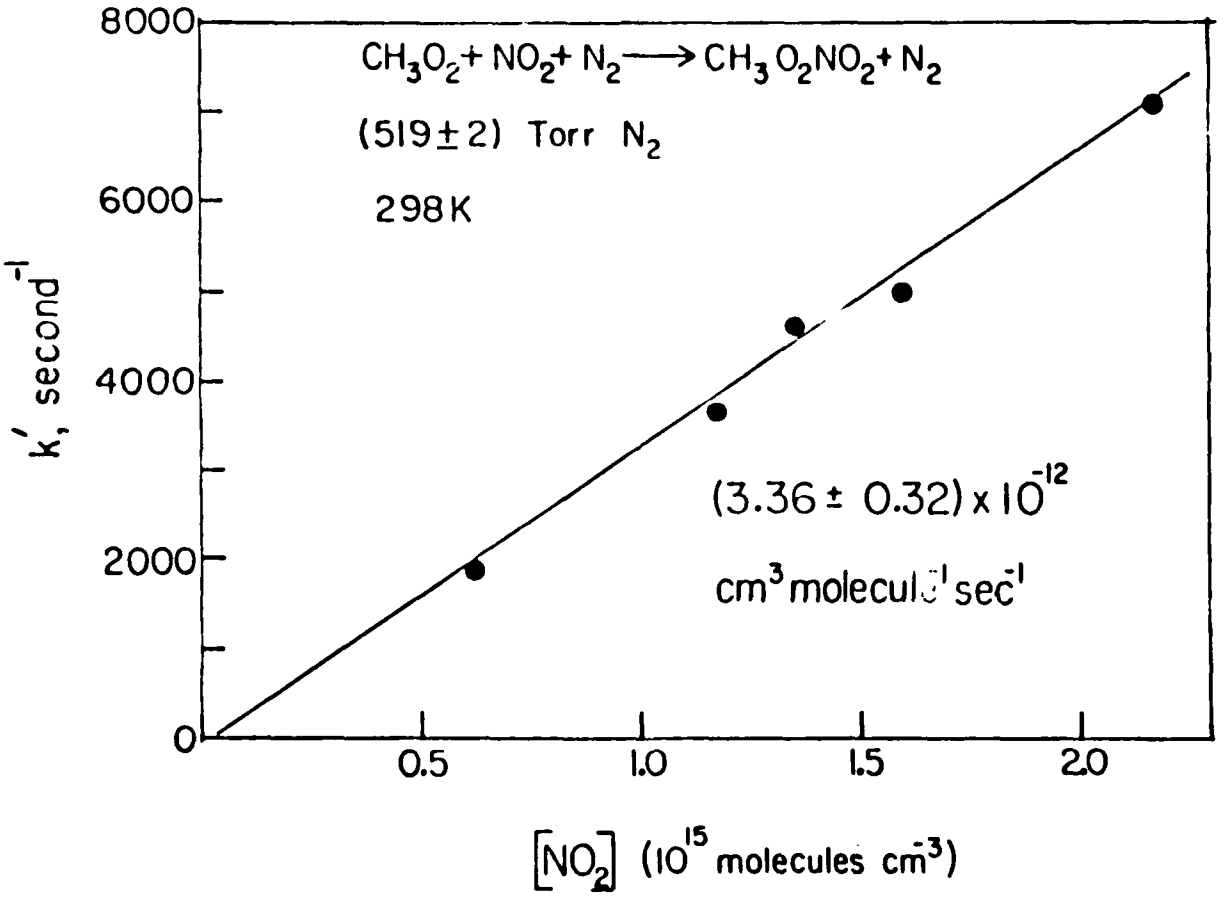

Figure 3. Plot of Pseudo-First Order Rate Constants vs. NO_2 Concentration at 298K and 519 torr of N_2.

Table I. Rate Constant Data for the Reaction of CH_3O_2 with NO_2.

Temperature K	N_2 Pressure torr	[Azomethane] 10^{15} cm^{-3}	$[O_2]$ 10^{17} cm^{-3}	$[CH_3O_2]_0$[a] 10^{13} cm^{-3}	$[NO_2]$ 10^{14} cm^{-3}	$k_f, 10^3 x s^{-1}$	$k_1 \times 10^{12}$[b] $cm^3 molecule^{-1} s^{-1}$
298	76±3	0.80	2.70	2.29	6.95	1.15	
		0.78	2.69	1.96	11.73	1.75	
		0.74	2.60	1.31	19.10	2.56	
		0.70	2.63	0.90	24.81	3.64	(1.36±0.23)
	157±2	0.52	4.50	1.13	7.94	1.50	
		1.52	4.34	1.22	10.08	1.70	
		0.53	4.34	1.00	14.96	2.82	
		0.81	4.40	2.33	17.54	3.12	
		0.53	4.47	0.99	21.47	4.05	(1.90±0.32)
	258±3	0.82	3.46	5.60	5.65	1.39	
		0.85	3.50	7.02	12.26	2.90	
		0.79	3.42	6.91	15.60	4.04	
		0.79	3.54	7.00	19.8	5.60	(2.60±0.56)
	352±3	0.77	3.53	2.56	6.87	1.88	
		0.71	3.52	3.39	9.42	2.70	
		0.79	3.52	2.46	11.88	3.70	
		0.67	3.50	2.32	13.63	3.77	
		0.73	3.51	2.66	16.05	4.50	(2.82±0.28)
	519±2	1.14	3.82	2.17	6.21	1.84	
		1.15	3.82	2.85	11.70	3.63	
		1.16	3.78	3.28	13.59	4.57	
		1.23	3.79	3.46	15.95	4.93	
		1.08	3.80	4.80	21.60	7.06	(3.36±0.32)
	722±1	0.821	5.68	3.75	5.38	1.91	
		1.76	5.66	4.00	7.47	2.60	
		0.843	5.68	4.70	9.86	3.42	
		0.88	5.66	5.90	12.79	4.95	
		0.91	5.66	3.20	15.92	6.15	(4.12±0.38)

Temperature K	N_2 Pressure torr	[Azomethane] 10^{15} cm^{-3}	$[O_2]$ 10^{17} cm^{-3}	$[CH_3O_2]_0$[a] 10^{13} cm^{-3}	$[NO_2]$ 10^{14} cm^{-3}	k_1', $10^3 x s^{-1}$	$k_1 \times 10^{12}$[b] cm^{3}molecule^{-1}s^{-1}
353	330±3	0.92	3.02	2.98	4.60	0.70	
		0.91	3.50	3.30	9.50	1.38	
		0.93	2.50	1.39	11.81	1.61	
		0.87	2.50	1.70	15.83	2.09	(1.19±0.15)
	354±2	0.96	4.57	2.22	8.64	1.42	
		0.86	4.56	1.97	15.32	2.27	
		1.03	4.56	1.35	24.73	3.81	
		0.79	4.53	1.03	30.21	4.22	(1.35±0.21)
	511±2	1.13	4.18	2.46	7.81	1.78	
		1.36	4.17	3.89	17.44	3.34	
		1.21	4.19	2.18	23.60	4.37	
		1.22	4.16	2.65	28.89	5.41	(1.71±0.10)
	696±2	1.11	4.76	2.23	9.94	2.28	
		2.08	4.69	3.57	20.70	4.17	
		1.74	5.00	3.12	24.12	5.27	
		1.46	4.73	1.71	31.71	6.81	
		1.62	4.73	2.41	4.50	8.84	(1.93±0.20)
253	109±1	1.30	3.60	1.53	2.77	1.05	
		1.39	4.56	1.55	4.02	1.44	
		1.32	3.60	1.62	5.75	2.03	
		1.31	3.70	1.82	7.56	2.36	
		1.31	3.80	0.89	9.16	2.86	
		1.31	3.70	1.31	11.10	3.10	(2.50±0.34)
	250±2	0.57	2.23	1.40	2.61	1.17	
		0.59	2.22	1.62	3.42	1.38	
		0.61	2.22	1.32	5.66	2.29	
		0.61	2.22	1.54	7.89	3.29	
		0.64	2.21	1.60	9.96	3.89	(3.85±0.30)

Temperature K	N_2 Pressure torr	[Azomethane] 10^{15} cm^{-3}	$[O_2]$ 10^{17} cm^{-3}	$[CH_3O_2]_0$[a] 10^{13} cm^{-3}	$[NO_2]$ 10^{14} cm^{-3}	k_1,10^3x s^{-1}	$k_1 \times 10^{12}$[b] cm^{3}molecule^{-1}s^{-1}
253	503±3	0.60	4.59	1.80	3.00	1.66	
		0.78	5.36	1.30	4.34	2.16	
		0.63	4.56	2.55	6.55	3.01	
		0.62	4.59	2.59	8.52	4.05	(5.10±0.50)
	519	1.11	5.22	2.2	5.85	2.60	
		0.99	5.21	2.6	11.20	5.72	
		0.88	5.21	2.0	18.15	9.72	
		1.10	5.22	2.1	23.8	13.20	(5.8±1.0)

a) The initial concentration of CH_3O_2, $[CH_3O_2]_0$, was calculated by back-extrapolating the decay curve for 150 μsec, (the delay between photolysis and initiation of signal acquisition.)

b) The quoted errors are 2σ and represent the precision of the measurements.

Table II. Rate Constants for the Reaction of CH_3O_2 with NO_2 as a Function of Temperature and N_2 Pressure.

Temperature K	Pressure torr	Number Density 10^{19} molecules cm^{-3}	$k_1 \times 10^{12}$ cm^3 molecule^{-1} s^{-1}
298	76	0.246	1.36 ± 0.23
	157	0.509	1.90 ± 0.32
	258	0.836	2.60 ± 0.56
	352	1.141	2.82 ± 0.28
	500	1.620	3.25 ± 0.50
	519	1.682	3.36 ± 0.32
	722	2.339	4.12 ± 0.38
353	330	0.903	1.19 ± 0.15
	354	0.966	1.35 ± 0.21
	511	1.398	1.71 ± 0.10
	696	1.904	1.93 ± 0.20
253	109	0.416	2.50 ± 0.34
	250	0.954	3.85 ± 0.30
	503	1.920	5.10 ± 0.50
	519	1.981	5.8 ± 1.0

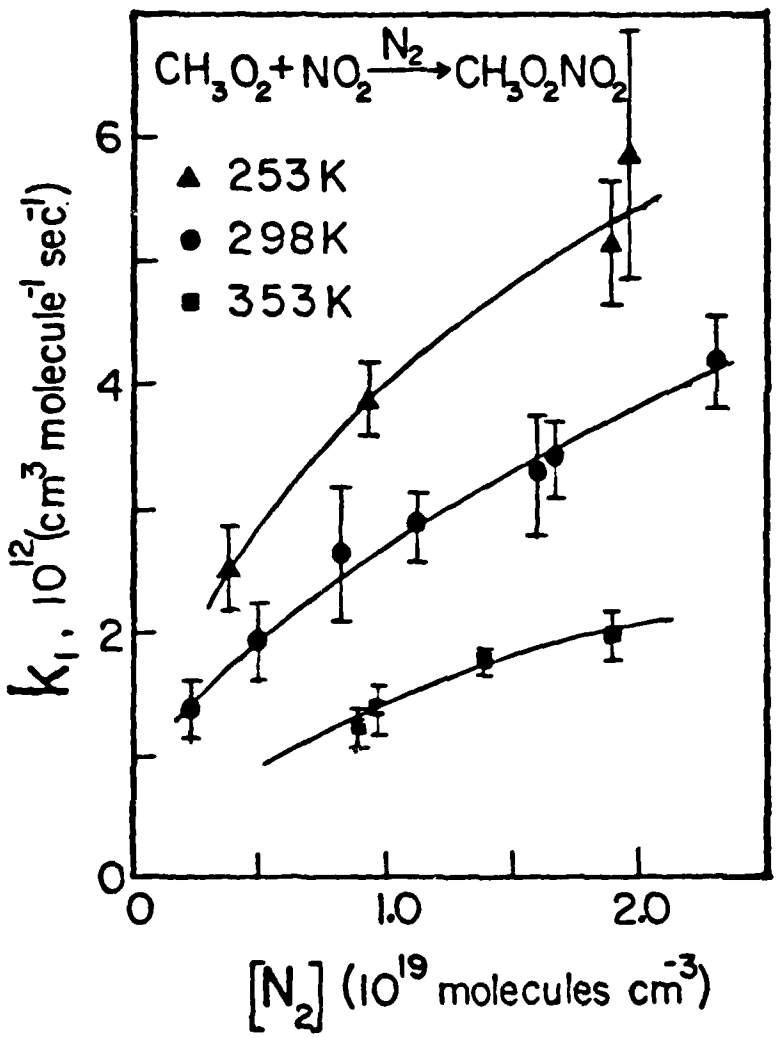

Figure 4. Plots of k_1 vs. N_2 Number Density. The lines drawn through the points are visual best fits.

There are two possible chemical complications that can arise in our experiments: (a) production of O_3 due to reaction of $O(^3P)$ (formed by either O_2 or NO_2 photolysis) with O_2 and (b) production of NO and its subsequent reaction with CH_3O_2. Photolysis of O_2 under the most unfavorable conditions, i.e., high $[O_2]$($\sim 5 \times 10^{17}$ cm^{-3}) and high photolysis laser energy ($\sim$ 10 mJ/cm^2), would produce $\sim 1 \times 10^{13}$ $O(^3P)$ cm^{-3}. (The absorption cross section for O_2 at 193 nm is $\sim 1 \times 10^{-21}$ cm^2.[13]) Similary, photolysis of NO_2 would lead to $\sim 1 \times 10^{13}$ $O(^3P)$ cm^{-3}. (The absorption cross section for NO_2 at 193 nm is $\sim 6 \times 10^{-19}$ cm^2[15].) Any $O(^1D)$ that is formed via photolysis would be quenched to $O(^3P)$ in less than 0.1 μsec by N_2.[16] The photolytically produced $O(^3P)$ would then react with either O_2 or NO_2,

$$O(^3P) + O_2 + M \xrightarrow{k_4} O_3 + M \qquad (4)$$

$$O(^3P) + NO_2 \xrightarrow{k_5} NO + O_2 \qquad (5)$$

The fraction of $O(^3P)$ that would lead to O_3 formation would, of course, depend on the ratio of $k_4[O_2][M]$ to $k_5[NO_2]$. Under the extreme conditions of low temperature (where k_4 is large) and low NO_2, we would produce $\sim 4 \times 10^{12}$ O_3 cm^{-3}. In our experiment, then, we would obtain $\sim$ 3% absorption of 257 nm radiation due to O_3. However, the O_3 formation does not affect measurement of the CH_3O_2 decay since all O_3 is formed within 100 μsec (99% completion) after the laser flash, and, therefore simply changes the value of I_0. The concentration of O_3 formed is too low to have any effect on the kinetics of the measured rate of CH_3O_2 decay. This conclusion was checked by increasing the photolysis energy by a factor of 4 while keeping $[CH_3O_2]_0$ constant (by decreasing [azomethane] by a factor

of 4); the measured decay rates were, within experimental error, unaffected.

The mount of NO that is produced via NO_2 photolysis would be at most 1.2% when 10 mJ/cm^2 is used for photolysis and all $O(^3P)$ that is produced reacts with NO_2 to produce NO. NO would of course, react with CH_3O_2 to produce CH_3O and NO_2,

$$CH_3O_2 + NO \xrightarrow{k_2} CH_3O + NO_2 \quad . \qquad (2)$$

The rate constant for Reaction (2) is known to be $\sim 8 \times 10^{-12}$ cm^3 molecule^{-1}s^{-1}.[1-3] Since the measured values of k_1 vary from 1.19 to 5.8×10^{-12} cm^{3}molecule^{-1}s^{-1}, the contribution of Reaction (2) could never be greater than 8% (i.e., at high temperature and low pressures). Again, this possibility was discarded as inconsequentialy by the observation that the measured rate constant was independent of photolysis energy. CH_3O formed in Reaction (2) would react with NO_2 to give CH_3ONO_2.

$$CH_3O + NO_2 \longrightarrow CH_3ONO_2 \quad . \qquad (6)$$

Formation of CH_3ONO_2 would not affect the measured rate constant since CH_3ONO_2 does not regenerate CH_3O_2, does not strongly absorb 257 nm radiation, and its concentration is too low to effectively remove CH_3O_2 via reaction. (The absorption cross section for CH_3ONO_2 is $\sim 4 \times 10^{-20}$ cm^2 at 257 nm.[17])

In addition to the two photolysis related problems that were discussed above, it is possible that our measured rate constants are incorrect if the thermal decomposition of the $CH_3O_2NO_2$ product leads to CH_3O_2 production on the same time scale as the measured CH_3O_2 decay,

$$CH_3O_2NO_2 \xrightarrow{M} CH_3O_2 + NO_2 \quad . \qquad (8)$$

Reaction (7) would, of course, be most severe at higher temperatures. The rate constant for Reaction (7) is not known. However, it cannot be very different from that of HO_2NO_2 decomposition leading to HO_2 and NO_2 production, which has been measured.[18] Using this rate constant, the fastest rate for Reaction (7) at 353K, would be $\sim 20s^{-1}$. This rate is negligible when compared to the $[CH_3O_2]$ decay rates of 699-8837 s^{-1} that were measured at 353K. Experimentally, if Reaction (7) was important, we would have observed non-exponential $[CH_3O_2]$ decays and more importantly, a non-linear dependence of k_1' on $[NO_2]$. We found the $[CH_3O_2]$ to decay exponentially for at least 3 1/e times and k_1' vs $[NO_2]$ plots were linear. Therefore, Reaction (7) could not have been significant under our experimental conditions.

Discussion

There are three separate direct measurements of k_1 at 298K. Cox and Tyndall[9] measured k_1 to be $(1.2 \pm 0.3) \times 10^{-12}$ $cm^3 molecule^{-1} s^{-1}$ at 500 torr of Ar + CH_4, and $k_1 = (1.6 \pm 0.3) \times 10^{-12}$ $cm^3 molecule^{-1} s^{-1}$ at 540 torr N_2, using the molecular modulation technique. This pressure independent value of k_1 is in good agreement with those obtained by Adachi and Basco[10] who measured k_1 to be $(1.53 \pm 0.07) \times 10^{-12}$ $cm^3 molecule^{-1} s^{-1}$ independent of pressure (between 53 and 580 torr Ar) using the method of flash photolysis-kinetic spectroscopy. This pressure independent behavior has been interpreted to mean that Reaction (1) is at its high pressure limit above $\sim$ 50 torr of Ar. Sander and Watson,[2] however, found k_1 to vary from $(1.5 \pm 0.10) \times 10^{-12}$ $cm^3 molecule^{-1} s^{-1}$ at 50 torr N_2 to $(3.94 \pm 0.17) \times 10^{-12}$ $cm^3 molecule^{-1} s^{-1}$ at 700 torr of N_2 at 298K. Moreover, the value of k_1 was observed to be dependent on the nature of the bath gas, i.e., He, N_2, or SF_6. This type of pressure dependent behavior is typical of an addition reaction. Sander and Watson's data also shows that Reaction (1) is in the "fall-off" regime, i.e., between second and third order, in pressure range of 50 to 700 torr of He, N_2, and SF_6. It should also be pointed out that the lower pressure values of k_1 obtained by Sander and Watson agree reasonably well with k_1 values of both Cox and Tyndall, and Adachi and Basco.

As seen from Table III, our measured values of k_1 are in excellent agreement with those of Sander and Watson; this argues very heavily for k_1 being pressure dependent. Sander and Watson have pointed out that the possible reason for the discrepancy between their values at higher pressures and those of Cox and Tyndall, is the long residence time of the gas mixtures and depletion of NO_2 along the length of the cell in

Table III. Comparison of Our Results With Previous Data at 298K.

		k_1, 10^{12} x $cm^3 molecule^{-1} s^{-1}$			
Pressure torr	Diluent	This Work	Sander and Watson* Ref (2)	Cox and Tyndall Ref (9)	Adachi and Basco Ref (10)
50	N_2		1.15±0.10		
76	N_2	1.36±0.23			
100	N_2		1.58±0.15		
157	N_2	1.90±0.32			
225	N_2		2.22±0.31		
258	N_2	2.60±0.56			
350	N_2		2.98±0.23		
352	N_2	2.82±0.28			
500	N_2	3.25±0.50	3.67±0.21		
519	N_2	3.36±0.32			
540	N_2			1.6±0.3	
700	N_2		3.94 ± 0.17		
722	N_2	4.12±0.38			
50	Ar+CH_4			1.2±0.3	
53-580	Ar				1.53±0.07

*The preferred value reported by Watson and Sander is the average value $\equiv k_1'/[NO_2]$.

the molecular modulation apparatus. In Adachi and Basco's experiments, the concentrations of reactants used were extremely large. This should have led to many secondary reaction complications. Also, their CH_3O_2 radical detection scheme was quite insensitive. Furthermore, as the authors pointed out, they would have to make a large correction to their high flash energy results due to the participation of Reaction (6), if $k_6 \approx 8 \times 10^{-12}$ $cm^3 molecule^{-1} s^{-1}$. To date, three separate direct measurements of k_6 have been carried out which yield a value of $k_6 = (8 \pm 2) \times 10^{-12}$ $cm^3 molecule^{-1} s^{-1}$.[1-3] Even though Adachi and Basco carried out a separate set of experiments using low flash energies and obtained values of k_1 (supposedly in the absence of secondary reaction complications) in agreement with their previous measurements, their results have to be considered suspect. They had very large concentrations of free radicals even in their low flash energy experiments which could lead to erroneous results. We believe that at 298K, the data obtained by Sander and Watson and in the present investigation are devoid of secondary reaction complications and hence should be used for atmospheric modeling studies.

There are no previous determinations of the temperature dependence of k_1. Our results are consistant with what is to be expected for an addition reaction which goes through an energy-rich complex. The strong temperature dependence of the measured values of k_1 suggests that $k_{1\infty}$ is likely to be $> 1 \times 10^{-11}$ $cm^3 molecule^{-1} s^{-1}$ at 253K. At 600 Torr, for example, the apparent "activation energy" for Reaction (6) is ~ -1.8 Kcal/mole.

For atmospheric modelling purposes it is convenient to obtain an analytical expression which best describes the temperature and pressure dependence of k_1. Sander and Watson have fit their data for k_1 at 298K

to the following semi-empirical equation which is based on Troe's formulation of RRKM theory:[19]

$$k([M],T) = \frac{k_c(T)[M]}{1 + \frac{k_c(T)[M]}{k_\infty(T)}} \; F_c^{\{1 + [\log_{10}(k_c(T)[M]/k_\infty(T))]^2\}^{-1}} \qquad (I)$$

$$k_c(T) = k_c(298)\left(\frac{T}{298}\right)^{-n}$$

$$k_\infty(T) = k_\infty(298)\left(\frac{T}{298}\right)^{-m} .$$

In Equation (I), $k_c(k_\infty)$ are the rate constants in the low (high) pressure limits and F_c is a parameter which relates the energy dependence of the rate constant for activated complex decomposition to the shape of the k vs [M] curve. They obtain $k_0(298) = (2.33 \pm 0.8) \times 10^{-30}$ cm^6 $molecule^{-1}sec^{-1}$, $k_\infty = (7.0 \pm 1.0) \times 10^{-12}$ cm^3 $molecule^{-1}$ sec^{-1} and $F_c = 0.4$. Because Sander and Watson's data base at 298K is much larger than ours and because our results are in excellent agreement with theirs, we have fit our temperature dependent data by trial and error with the constraint that $k_0(298)$, $k_\infty(298)$, and F_c must fall within the error limits given by Sander and Watson. The best fit to the data is obtained for (Figure 4)

$$k_0(T) = 2.2 \times 10^{-30}\left(\frac{T}{298}\right)^{-2.5} \; cm^6 molecule^{-2}s^{-1}$$

$$k_\infty(T) = 7 \times 10^{-12}\left(\frac{T}{298}\right)^{-3.5} \; cm^3 molecule^{-1}s^{-1}$$

$$F_c = 0.4 .$$

Our results suggest that Reaction (1) could contribute significantly towards removal of CH_3O_2 and NO_2 in the presence of high concentrations of NO_x (such as those encountered in urban smog) if $CH_3O_2NO_2$ is thermally stable.

References

1. I.C. Plumb, K.R. Ryan, J.R. Steven, and M.F.R. Mulcahy, Chem. Phys. Letters 63, 255 (1979).

2. S.P. Sander and R.T. Watson, J. Phys. Chem. (in press).

3. A.R. Ravishankara, F.L. Eisele, and P.H. Wine, presented at the Gordon Conference on Environmental Chemistry—Air, 1979.

4.(a) C.J. Howard and K.M. Evenson, Geophys. Res. Lett. 4, 437 (1977).

(b) B.Reimann and F. Kaufman, paper presented at 13th Informal Conference on Photochem., Clearwater Beach, FL (1978).

(c) J.P. Burrows, D.I. Clift, G.W. Harris, B.A. Thrush, and J.P. Wilkinson, W.M.O. Sym. Ozone, Toronto, Canada (1978).

(d) J.J. Margitan and J.G. Anderson, paper presented at 13th Informal Conference on Photochemistry, Clearwater Beach, FL (1978).

(e) M.T. Leu, J. Chem. Phys. 70, 1662 (1979).

5. C.J. Howard, J. Chem. Phys. 71, 2352 (1979).

6.(a) C.W. Spicer, A. Villa, H.A. Wiebe, and J. Heicklen, J. Amer. Chem. Soc. 95, 13 (1973).

(b) R. Simonaitis and J. Heicklen, J. Phys. Chem. 78, 2417 (1974).

(c) R. Simonaitis and J. Heicklen, J. Phys. Chem. 79, 298 (1975).

7. C.T. Pate, B.J. Finlyason, and J.N. Pitts, Jr., J. Amer. Chem. Soc. 96, 6554 (1974).

8. R.A. Cox, R.G. Derwent, P.M. Holt, and J.A. Kerr, J.C.S. Faraday I, 72, 2444 (1976).

9. R.A. Cox and G.S. Tyndall, Chem. Phys. Lett. 65, 357 (1979).

10. H. Adachi and N. Basco. Int. J. Chem. Kinet. XII, 1 (1980).

11. P.H. Wine, N.M. Kreutter, and A.R. Ravishankara, J. Phys. Chem. 83, 3191 (1979).

12. A.M. Bass, A.E. Ledford, Jr., and A.H. Laufer, J. Res. Natl. Bur. Stand. Section A 80, 143 (1976).

13. J.G. Calvert and J.N. Pitts, Jr., "Photochemistry," John Wiley and Son, Inc. 1966.

14. S.P. Sander and R.T. Watson, Private communications, 1980.

15. H.S. Johnston, S.G. Chang, and G. Whitten 78, 1 (1974).

16. NASA Reference Publication 1049, "The Strantosphere: Present and Future," Editors, R.D. Hudson and E.I. Reed, (1979).

17. W.D. Taulor, T.D. Allston, M.J. Moscato, G.B. Fazekas, R. Kozlosi, and G.A. Takacs, Int. J. Chemical Kinetics, in press, 1980, and references therein.

18. R.A. Graham, A.M. Winer, and J.N. Potts, Jr., J. Chem. Phys. 68, 4505 (1978).

19. J. Troe, J. Phys. Chem. 83, 114 (1979).
J. Troe, J. Chem. Phys. 66, 4758 (1977).

Acknowledgements

We would like to thank Drs. S.P. Sander and R.T. Watson for very helpful discussions throughout this work. We would also like to thank Mr. A.O. Langford for discussions which steered us towards utilization of colinear photolysis and probing laser beams.

This work was supported by the U.S. Department of Transportation/ Federal Aviation Administration through Contract #DOT-FA76WA-4259.

Chapter 2

A STUDY OF OH REACTION WITH HNO_3: KINETICS AND NO_3 YIELD

INTRODUCTION

Nitric acid, HNO_3, is an important reservoir for both HO_x and NO_x species in the stratosphere where it is principally formed via the combination reaction of NO_2 with OH,

$$OH + NO_2 + M \xrightarrow{k_1} HNO_3 + M \quad . \tag{1}$$

HNO_3 is removed from the stratosphere via solar photolysis as well as reaction with OH,

$$OH + HNO_3 \xrightarrow{k_2} \text{products} \quad . \tag{2}$$

Recently, we measured k_2[1] and found it to be faster than previously believed.[2-5] In addition, k_2 was found to exhibit a negative temperature dependence which is unusual for a biomolecular reaction. Even though it is known that NO_3 is formed in reaction (2) at 298 K[6] and it has been generally assumed that NO_3 and H_2O are the only products of reaction (2), we suggested the possibility of reaction (2) proceeding through multiple pathways leading to different sets of products,[1] i.e.,

$$OH + HNO_3 \xrightarrow{k_{2a}} H_2O + NO_3 \tag{2a}$$

$$OH + HNO_3 \xrightarrow{k_{2b}} H_2O_2 + NO_2 \tag{2b}$$

$$OH + HNO_3 \xrightarrow{k_{2c}} \text{Addition Product} \tag{2c}$$

It was further implied that the branching ratios, i.e., k_{2a}/k_2 and k_{2b}/k_2 could vary with temperature, thereby explaining the unusual temperature dependence.

In stratospheric model calculations it was found that the estimated ozone concentration changes due to anthropogenic emissions were sensitive to not only the new value of k_2 but also the identity of the reaction products. Therefore, we carried out the experiments reported here to measure the yield of NO_3 in reaction (2) as well as to remeasure k_2 by a different experimental technique. The rate coefficient was measured by monitoring the temporal profile of NO_3 formed from reaction (2) following the production of OH by laser photolysis of HNO_3. By measuring the amount of NO_3 produced from a known (calculated) concentration of OH, the yield of NO_3 and hence the branching ratio, k_{2a}/k_2, was also determined.

While the work reported here was in progress, three other groups have studied reaction (2). Nelson et.al.[7] measured k_2 at 298 K using flash photolysis-resonance fluorescence technique to be $(8.2 \pm 1.8) \times 10^{-14}$ $cm^3 molecule^{-1} s^{-1}$ and using flash photolysis-laser absorption technique to be $(10.6 \pm 3.4) \times 10^{-14}$ $cm^3 molecule^{-1} s^{-1}$. In addition, they also found the NO_3 free radical to be a major product of reaction (2). Kurylo et.al.[8] and Margitan and Watson[9] have also studied reaction (2) using the flash photolysis-resonance fluorescence technique. Their results are in reasonably good agreement with our previous measurements both in terms of the observation of a negative temperature dependence and the value of k_2 at 298 K (and other temperatures).

EXPERIMENTAL

The experimental approach used in the present investigation of reaction (2) was to create OH via pulsed laser photolysis of HNO_3, and to subsequently monitor the temporal concentration profile of the NO_3 reaction product using the long path laser absorption technique. Even if NO_3 is a minor product, as long as it is formed directly from reaction (2), the temporal profile

will reflect the rate of reaction (2). The ratio of $[NO_3]$ formed to initial [OH] is a direct measure of the branching ratio for NO_3 formation, k_{2a}/k_2.

A schematic diagram of the apparatus is shown in Figure 1. A jacketed pyrex cell $\sim$ 5 cm in diameter and $\sim$ 45 cm long was maintained at a fixed temperature using an ethylene glycol-water mixture circulated from a thermostated reservoir. HNO_3 mixed with a large amount of an inert gas (N_2, Ar or SF_6) was passed into the reactor and then into a (76 cm long) absorption cell. The concentration of HNO_3 in this mixture was directly measured in the absorption cell at 298 K using the 228.8 nm Cd line. The 228.8 nm line was isolated from the neighboring 214 nm line using a 0.25 m monochromator and detected by a photomultiplier tube (RCA 4837). The current output of the photomultiplier was constantly monitored using an electrometer. Before each run the cell was flushed with the diluent gas and I_o, the incident light intensity, recorded. Then, the HNO_3/diluent gas mixture was introduced and I, the transmitted light intensity, measured. At the end of the run, I_o was again measured to check for drifts in light intensity during the experiment. The HNO_3 concentration was calculated using an absorption cross section of 6.32×10^{-20} cm^2 at 228.8 nm.[10,11] The pressure in the system was measured at the exit of the reactor using a capacitance manometer. The flow rates of all gases were monitored using calibrated mass flow meters.

A pulsed KrF excimer laser (248 nm) was used as the photolysis light source. It was placed $\sim$ 2 m from the reactor to ensure a spatially uniform beam. The laser beam entered the reactor through mirror M_2 and exited through M_1 where its energy could be monitored. The cw 662 nm laser beam used for NO_3 concentration measurement was generated by pumping a tunable ring dye laser with the all-lines output of an argon ion laser. The line

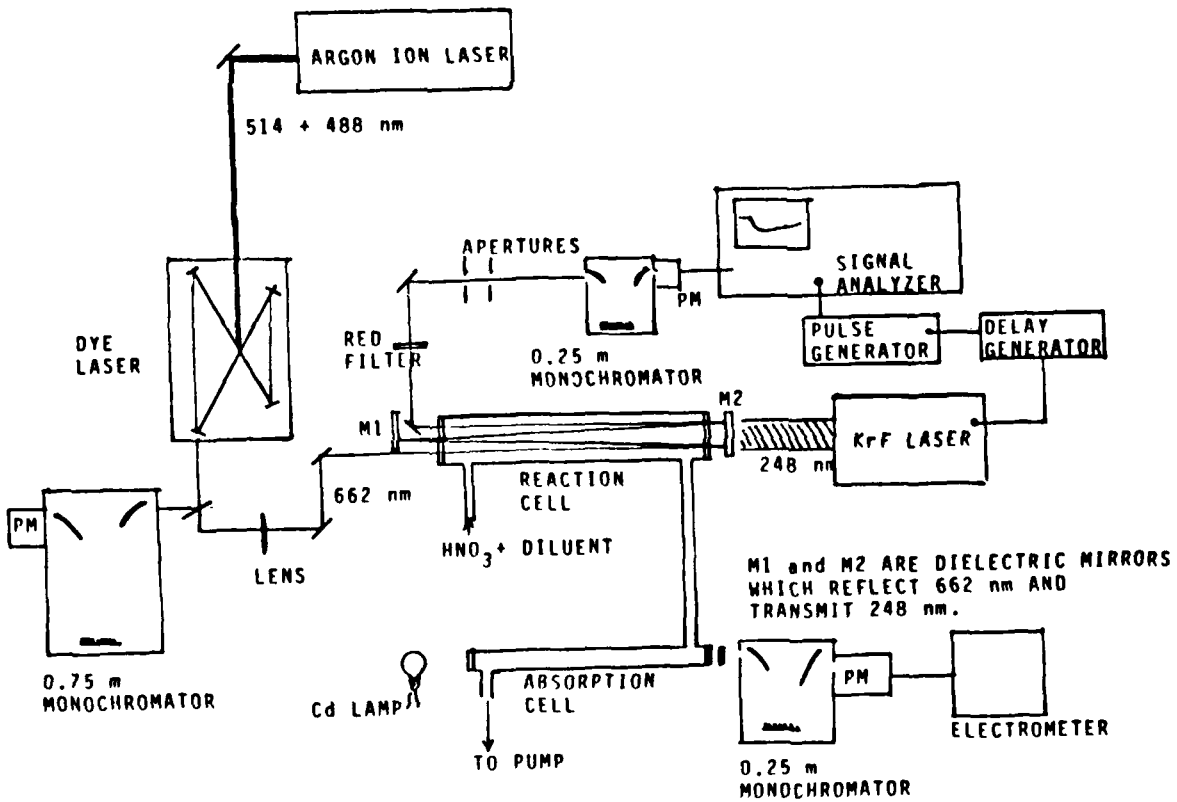

Figure 1. Schematic Diagram of the Laser Photolysis-Long Path Laser Absorption Apparatus.

width of the dye laser output was measured with a [illegible] etalon to be $\sim 2 \times 10^{-3}$ nm. The probe beam was multi-pass through the reactor using mirrors M_1 and M_2 to obtain a path length of 4.5 to 9 m (Mirrors M_1 and M_2 were specially coated to transmit 86% at 248 nm and reflect 99.5% at 660 nm). The probe beam emerged from the cell, passed through a red filter and a set of collimators and illuminated a diffuser attached to the entrance slit of a 0.25 m monochromator. A red-sensitive photomultiplier tube (Hamamatsu R928P) was used at the exit slit for light detection. The photomultiplier was wired so as to have a response time of less than 1 μsec and the resistor bridge current was always much greater ($\sim$ 1000 times) than the anode current. The photomultiplier response was found to be linear over a wide range of light intensity. The red filter prevented the detection of the photolysis beam while the combination of apertures, the diffuser, and the monochromator ensured that only the probe beam was detected (i.e., any fluorescence induced by photolysis laser and room light did not interfere with the measured probe beam intensity). The wavelength of the probe beam was periodically checked using a 0.75 nm monochromator operating in the second order. The monochromator was calibrated against known standards and the wavelength was accurate to 0.1 nm.

The diluent gases used in this study were obtained from Matheson Gas Products and had the following stated purities: Ar $\geq$ 99.995%, $SF_6 \geq$ 99.99% and $N_2 \geq$ 99.9995%. They were used without further purification. HNO_3 was prepared by reacting concentration H_2SO_4 wth $NaNO_3$ under vacuum at $\sim$ 290 K and collecting the vapor at 77 K. It was then purified by trap-to-trap distillation (273-77 K) with only the middle fraction being kept. The pure HNO_3 was stored in the dark at 77 K

In a typical kinetics experiment $\sim 10^{16} - 10^{17}$ HNO_3 cm^{-3} in 20-100 torr diluent gas (N_2, Ar, or SF_6) was flowed through the cell with a linear velocity of $\sim$ 3 cm/sec. The signal averager (working in the peak height analysis mode), which monitored the probeam intensity, was pretriggered $\sim$ 1 msec before the photolysis laser beam entered the reactor. Pretriggering allowed the measurement of I_o, the intensity of the 662 nm beam in the absence of NO_3. The photolysis laser beam (248 nm, $\sim$ 5 mJ cm^{-2}) photodissociated HNO_3 to produce OH,

$$HNO_3 \xrightarrow[\lambda=248nm]{h\nu} OH + NO_2 \quad . \tag{3}$$

OH then reacted with HNO_3 to produce NO_3;

$$OH + HNO_3 \xrightarrow{k_{2a}} H_2O + NO_3 \quad . \tag{2a}$$

The probe beam intensity was attenuated due to absorption by NO_3 and was measured in real time. This intensity-time profile was converted to an $[NO_3]$ time profile using the relationship $\ell n\ (I_o/I) = [NO_3]\sigma\ell$ (where σ is absorption cross section of NO_3 at 662 nm, and ℓ is the path length). One such profile obtained by averaging 32 flashes is shown in Figure 2. In general, 16-100 flashes (repetition rate .03 Hz) were averaged to obtain the NO_3 temporal profile. In the absence of any NO_3 loss, which was indeed the case when the reactor was completely replenished between photolysis laser flashes, the temporal profile of $[NO_3]$ is given by the relationship,

$$[NO_3]_t = \frac{k_{2a}}{k_2} [OH]_o \{1 - e^{-k_2[HNO_3]t}\}$$

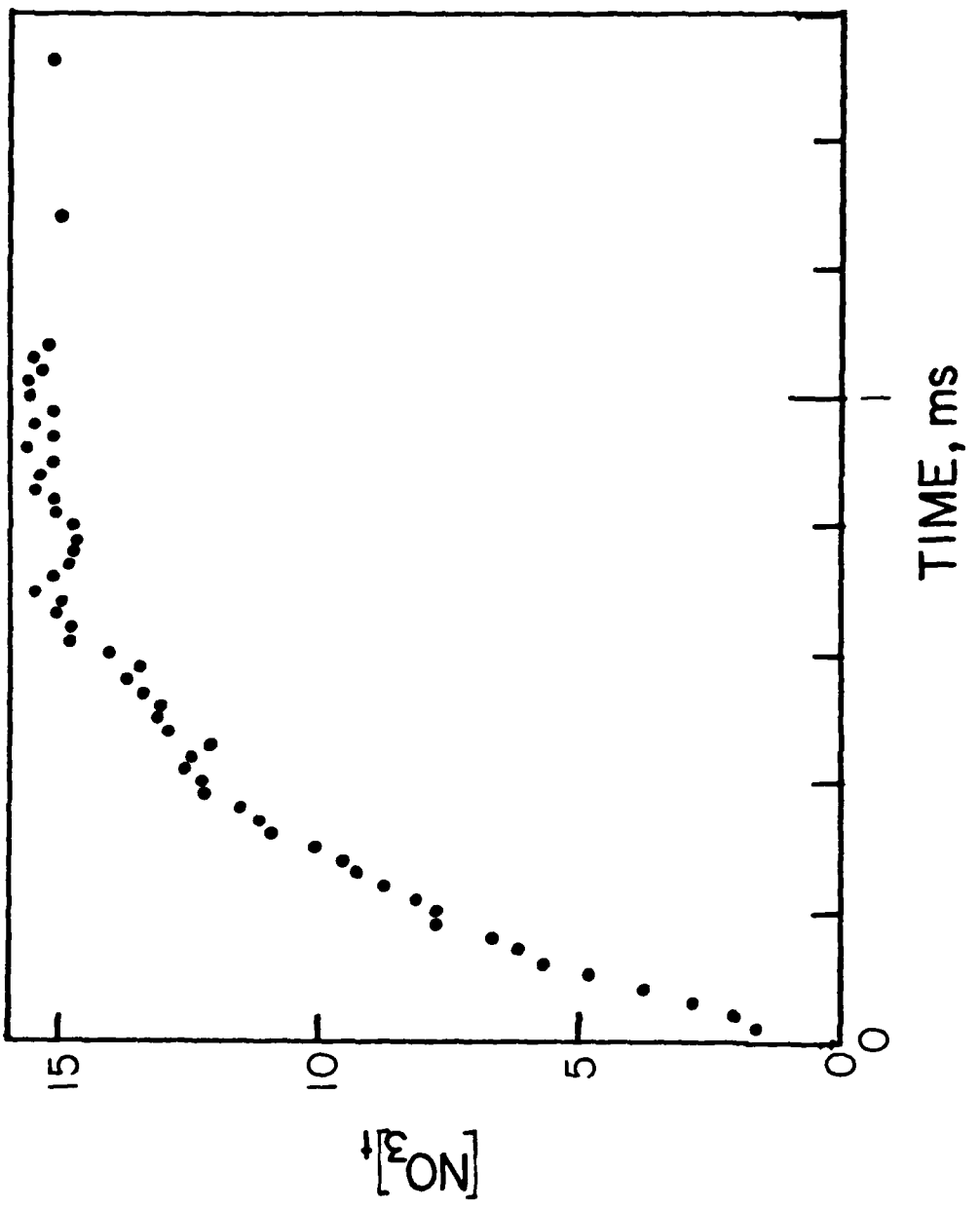

Figure 2. Temporal Profile of NO_3 Concentration Following the Photolysis of HNO_3 at 248 nm.

where $[NO_3]_t$ is concentration of NO_3 at time t, $[OH]_o$ is the initial [OH], and $[HNO_3]$ is the constant measured concentration of HNO_3. A plot of $\ell n\{[NO_3]_\infty - [NO_3]_t\}$ vs. time yields a straight line, such as the one shown in Figure 3; the slope of the line gives k_2' ($\equiv k_2[HNO_3]$). Note that to obtain k_2' neither σ nor ℓ needs to be known. k_2' was measured at various concentrations of $[HNO_3]$; a plot of k_2' vs. $[HNO_3]$ yields a straight line whose slope is k_2 (see Figure 4). (In most experiments, the $[NO_3]$ time profile was fitted using an iterative computer program to the expression

$$[NO_3]_t = \frac{k_2'}{k_d - k_2'} [OH]_o (k_{2a}/k_2) \{e^{-k_2't} - e^{-k_dt}\}$$

The value of k_2' thus obtained was identical to the slopes of $\ell n\{[NO_3] - [NO_3]_t\}$ vs. t plots since k_d, the first order rate constant for NO_3 loss, was usually $\sim 20\ s^{-1}$ while k_2' ranged from 3000 s^{-1} to 20,000 s^{-1}.

Experiments carried out to measure the yield of NO_3 in reaction (2) were very similar to the kinetics runs. Careful attention was given to ensure reproducibility in photolysis laser energy and beam quality. Unlike the kinetics runs only 10 flashes were averaged. The laser energy density was measured before and after the run using a calibrated energy monitor. In preliminary experiments it was determined that the energy density was constant to within 10% over the whole length of the cell. The transmission of the mirror M_2 and cell windows were directly determined by measuring the attenuation of the 248 nm laser beam. As in the kinetics runs the concentration of HNO_3 was constantly monitored. The maximum in absorption due to NO_3 was measured for various concentrations of HNO_3 and laser energies. Since, there was no loss of NO_3 in the time scale of the experiment, the maximum absorbance gave the net concentration of NO_3 produced. The initial

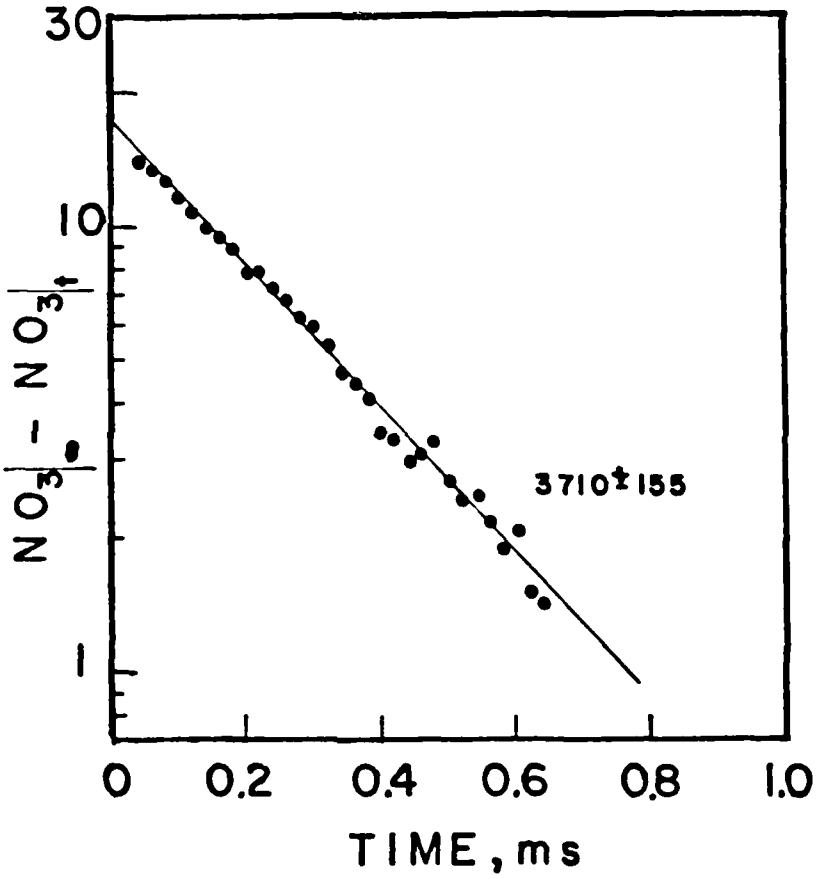

Figure 3. First Order NO_3 Growth Plot; Slope of the Line Gives k'.

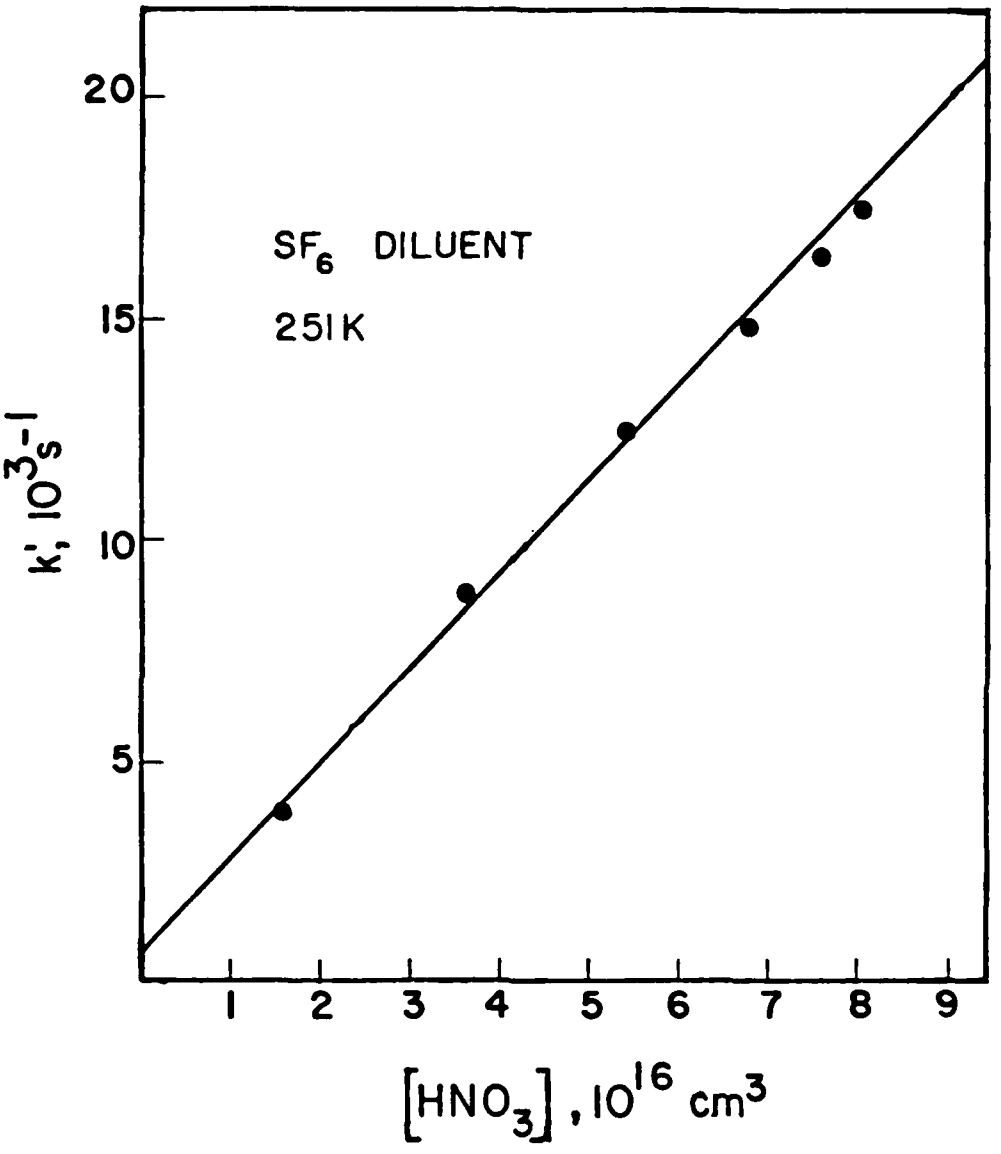

Figure 4. Plot of k' vs. HNO_3 Concentration Slope Gives the Rate Coefficient.

concentration of photolytically produced OH, $[OH]_o$, was calculated using the equation,

$$[OH]_o = P \times [HNO_3] \times \sigma^{248}_{HNO_3} \times \Phi$$

where P = photon flux at 248 nm in photons/cm^2, $[HNO_3]$ is the measured HNO_3 concentration, $\sigma^{248}_{HNO_3}$ is the absorption cross section of HNO_3 at 248 nm taken to be 2.01 x 10^{-20} cm^2/molecule,[10,11] and Φ is the quantum yield of OH in HNO_3 photolysis at 248 nm and taken to be unity.[12] (This equation is valid since the system is optically thin at 248 nm.) The concentration of NO_3 produced was calculated using the relation,

$$[NO_3]_{max} = \frac{1}{\sigma^{662}_{NO_3} \ell} \ln(I_o/I_m)$$

where I_o and I_m are measured intensities of 662 nm beam in the absence and the presence (at maximum) of NO_3, σ^{662}_{NO3} is the absorption cross section for NO_3 at 662 nm taken to be 1.70 x 10^{-17} cm^2[13,14,15] and ℓ is the path length. The ratio $[NO_3]_{max}/[OH]_o$ gives the yield of NO_3 in reaction (2).

RESULTS AND DISCUSSION

Some initial tests were performed to ensure that the absorption at 662 nm was indeed due to NO_3. When the laser was tuned off the band no absorption was measured. When tuned on to the side of the band, an absorption that is to be expected (within 20%) based on the reported cross sections was measured.[13-15] In addition, it was verified that NO_2 and HNO_3 were not contributing to the measured attenuation. Therefore, it is clear that NO_3 was indeed the transient that was measured.

Kinetic Studies

All experiments were carried out under pseudo-first order conditions with HNO_3 in very large excess ($10^3 < [HNO_3]/[OH]_o < 5 \times 10^4$). In preliminary experiments it was determined that a variation of 10 in $[HNO_3]/[OH]_o$ ratio at a fixed $[HNO_3]$ did not affect the measured rate coefficients. Also, as long as the contents of the reactor were completely replaced between consecutive photolysis laser flashes, the NO_3 concentration reached a maximum and its subsequent decay rate was very small. The position of the absorption cell (i.e., in front or back of the reaction with respect to the direction of gas flow) did not have any effect on the measured rate coefficient. As seen from Figure 3, the decay of [OH] as reflected by the $[NO_3]$ rise is exponential and the dependence of $k_2'(\equiv k_2[HNO_3])$ on $[HNO_3]$ is linear. These observations in conjunction with the invariance of k_2 to changes in $[OH]_o$, i.e., photolysis laser energy, demonstrate that chemical complications did not effect the measured value of k_2.

One systematic error which can produce the observed negative temperature dependence of k_2 is the occurrence of reaction (2) due to the presence of NO_2 in the HNO_3 sample or in the reactor. Concentrations of NO_2 in our HNO_3 samples were unmeasurably low. (NO_2 concentration was measured using long path absorption of 366 nm.) (Note that one needs $\sim$ 20% NO_2 in the sample to see the observed increase with decrease in temperature while the upper limit for measured NO_2 was 0.5%.) In addition, we checked for the presence of reaction (1) by taking advantage of the fact that k_1 is strongly dependent on both pressure and the identity of the third body.[16] As seen from Table I, the pressure and identity of the third body did not effect the measured value of k_2. It is easy to show that if reaction (1) was indeed important substantial differences in measured values of k_2 would have been observed.

Table I

$k_2 \times 10^{13}$, $cm^3 molecule^{-1} s^{-1}$

Temperature, K / Diluent	298		251	
Ar, 50 torr	1.25	0.13	-----	
N_2, 50 torr	-----		1.94	0.24
SF_6, 60 torr	1.39	0.28	2.09	0.17

Figure 5 shows the Arrhenius plot for reaction (2). As seen from this figure, the present measurements yield k_2 values which are in excellent agreement with our previous measurements. (We could not measure k_2 at temperatures much lower than 251 K because the vapor pressure of HNO_3 is very low and hence sufficient concentrations of HNO_3 could not be introduced into the cell to perform the measurement. It should be noted that the concentrations of HNO_3 needed in the current method are $\sim$ 20 times larger than those required in our previous flash photolysis-resonance fluorescence experiments.[1]) Discrepancies between our values of k_2 and other previous (pre 1980) measurements have already been described.[1] Hence no discussion of these discripancies needs to be presented here.

Of the three recent measurements of k_2 at 298 K, only the results of Nelson et.al.[7] seen to be different from our measured value of k_2. Their value of k_2 measured using the flash photolysis-laser absorption technique, $(1.0 \pm 3.4) \times 10^{-14}$ $cm^3 molecule^{-1} s^{-1}$, falls within the lower limits of the k_2 values of our two studies, $(12.5 \pm 2.8) \times 10^{-14}$ and $(13.2 \pm 3.0) \times 10^{-14}$ $cm^3 molecule^{-1} s^{-1}$. However, their k_2 value obtained using a technique very similar to our previous study yields the lowest value of k_2 reported since 1980. There are no obvious reasons as to why Nelson et.al.'s results disagree with k_2 values reported by Kurylo et.al.,[8] 1.38×10^{-13} $cm^3 molecule^{-1} s^{-1}$, Margitan and Watson,[9] 1.1×10^{-13} $cm^3 molecule^{-1} s^{-1}$, and our two measurements.

The temperature dependencies observed by Kurylo et.al.[8] and Margitan and Watson[9] are very similar to that observed by us previously. However, both these studies tend to support a non-Arrhenius behavior of k_2, k_2 not decreasing with increases in temperature at $T > 298$ K. Kurylo et.al. have fit their low temperature (i.e., $T < 298$ K) data to an Arrhanius form,

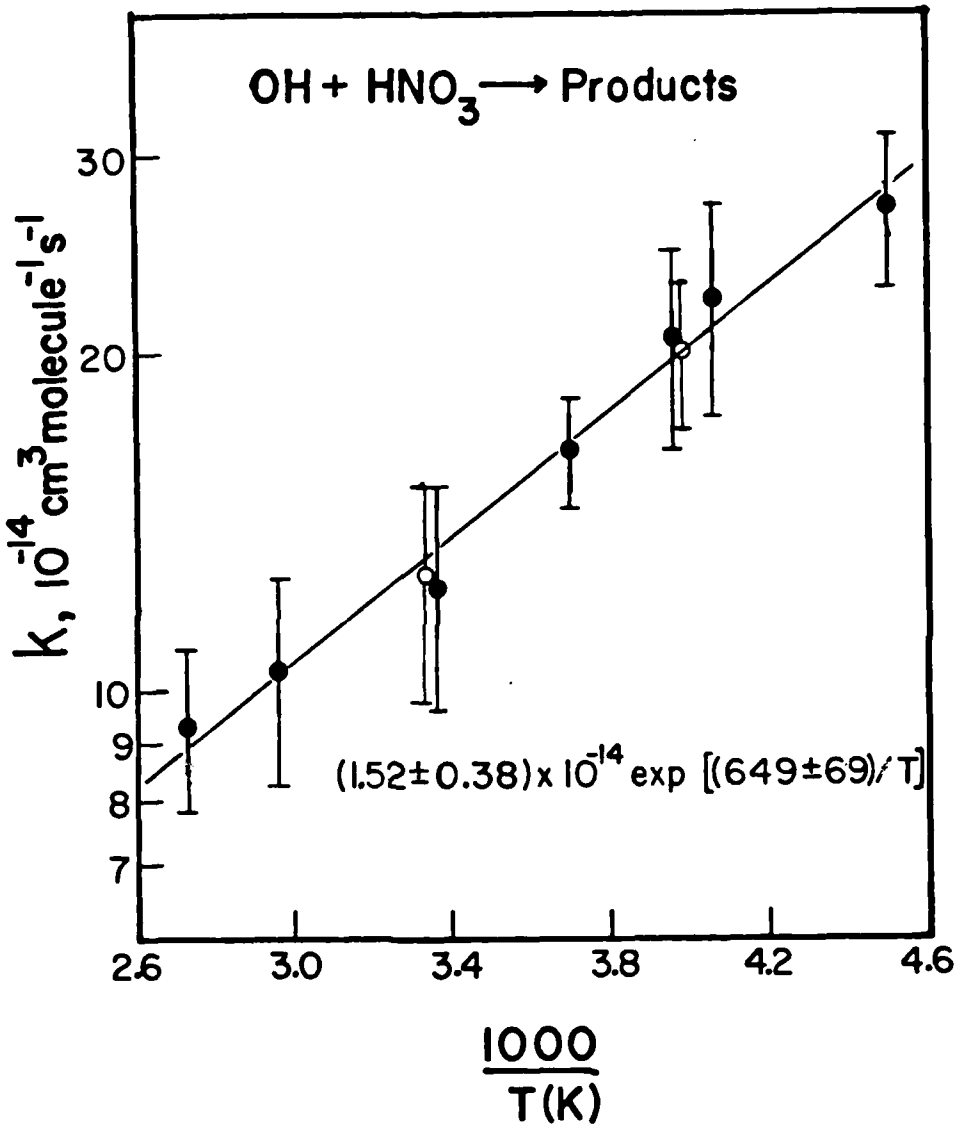

Figure 5. Arrhenius Plot of k_1. Open Circles Obtained by Monitoring NO_3. Close Circles from our Previous Study (Wine et.al., JGR, 86, 1105 (1981).

$$k_2 = (1.05 \pm 0.20) \times 10^{-14} \exp[\frac{760 \pm 50}{T}] \text{ cm}^3\text{molecule}^{-1}\text{s}^{-1},$$

which is nearly identical to that reported by us previously. Margitan and Watson have chosen not to report an Arrhenius expression since they observe a slight change in k_2 when pressure is changed from 20-100 torr at 238 K. They believe that the pressure dependence of k_2 is real since there was insufficient amount of NO_2 in their system for reaction (1) to be responsible for this observation.

NO_3 Yield in Reaction 2

As in the case of kinetics experiments the yield measurements were carried out under pseudo-first order conditions. The ratio of the NO_3 yield to the initial OH concentration $[NO_3]/[OH]_o$, was measured. At 298 K the average of 7 runs yield $[NO_3]/[OH]_o$ to be (0.98 ± 0.20) and an average of 5 runs at 251 K yield the ratio to be (1.17 ± 0.19). The quoted errors are 2σ and refer to the precision only. A propagation of error calculation was carried out to estimate systematic errors. The major source of systematic errors are inaccuracies in photolysis photon flux measurements and in the absorption cross sections for NO_3 at 662 nm and HNO_3 at 248 and 228.8 nm. The yields are calculated to be 0.97 ± 0.35 at 298 K and 1.17 ± 0.34 at 251 K. (These errors represent 2σ values.) The lower limits for NO_3 yields are, therefore, 0.62 and 0.83 at 298 K and 251 K, respectively.

The yield measurements demonstrate clearly that NO_3 is the major, if not the only, product of reaction (2) (i.e., k_{2a}/k_2 is close to unity). This result is not surprising and confirms the previous assumption regarding the reaction pathway. Even though the yields at 298 K and 251 K are, within quoted errors, identical, a possible source of discrepancy between the two

measurements needs to be pointed out. It has been assumed that the NO_3 absorption cross section at 662 nm, $\sigma^{662}_{NO_3}$, is temperature independent—an assumption that is not proven. Any such temperature dependence will directly effect the measured value. The second possible source of error is the absorption cross section of HNO_3 at 248 nm being temperature dependent. We have shown that there were no secondary chemistry problems. In this regard, it should be noted that secondary chemistry (which should be due to either secondary reaction which consume OH or NO_3) would tend to reduce the yields, but the measured yields are around the theoretical maximum. It should be pointed out that our measured value of NO_3 yield is in good agreement with the results of Nelson et.al.

CONCLUSIONS

The results of the present study confirm our previous value of k_2 at 298 K as well as the temperature dependence of k_2. Two other flash photolysis studies, by Kurylo et.al.[8] and Margitan and Watson,[9] also are in good agreement with our previous results as well as the present values of k_2. However, the results of Nelson et.al.[7] at 298 K do not agree with these four studies. The yield measurements demonstrate that reaction (2a) is the major pathway and is in agreement with results of Nelson et.al. Thus the atmospheric calculation presented earlier[1] assuming NO_3 to be the only product can be considered preferable over the other alternative. The maximum affects on perturbation calculations due to the new values of k_2 seems most reasonable.

Finally, it should be pointed that there could, eventually, be a good agreement between various measurements thereby increasing our confidence in atmospheric chemistry calculations. However, until a good feasible explanation of the origin of the unusual temperature dependence of k_2 is

available, reaction (2) will not be well understood and a certain level of caution (skeptcism?) should be exercised in applying these results to atmospheric calculations.

References

1. P.H. Wine, A.R. Ravishankara, N.M. Kreutter, R.C. Shah, J.M. Nicovich, R.L. Thompson, and D.J. Wuebbles, J. Geophys. Res. 86, 1105 (1981).

2. R. Zellner and I.W.M. Smith, Chem. Phys. Lett. 26, 72 (1974).

3. I.W.M. Smith and R. Zellner, Int. J. Chem. Kinet. Symp. 1, 341 (1975).

4. J.J. Margitan, F. Kaufman, and J.G. Anderson, Int. J. Chem. Kinet. Sym. 1, 281 (1975).

5. R. Hudson and E.I. Reed (Eds.), NASA Ref. Publ. 1049 (1979).

6. D. Husain and R.G.W. Norrish, Proc. R. Soc. London, Ser. A., 273, 165 (1963).

7. H.H. Nelson, W.J. Marinelli, and H.S. 495 (1981).

8. M.J. Kurylo, K. Cornett, and J. Murphy, J. Geophys. Res., to be submitted, 1981.

9. J.J. Margitan and R.T. Watson, 182nd ACS National Meeting, August 23-28, New York, New York, 1981.

10. H.S. Johnston and G. Graham, J. Phys. Chem. 77, 62 (1973).

11. F. Biaume, J. Photochem. 2, 139 (1973).

12. H.S. Johnston, S. Chang, and G. Whitten, J. Phys. Chem. 78, 1 (1974).

13. R.A. Graham and H.S. Johston, J. Phys. Chem. 82, 254 (1978).

14. D.N. Mitchell, R.P. Wayne, P.J. Allen, R.P. Harrison, and R.J. Twin, J. Chem. Soc. Faraday V, 76, 785 (1980).

15. F. Magnotta and H.S. Johnston, Geophys. Res. Lett. 7, 769 (1980).

16. P.H. Wine, N.M. Kreutter, and A.R. Ravishankara, J. Phys. Chem. 83, 3191 (1979).

ACKNOWLEDGEMENT:

We would like to thank C.A. Gump and N.M. Kreulter for their help in preparing HNO_3. We would also like to thank Drs. M.J. Kurylo and J.J. Margitan for communicating to us their results prior to publication.

This work was supported by the U.S. Department of Transportation/ Federal Aviation Administration through Contract Number DOT-FA-78WA-4259.

APPENDIX I

Preparation of Azomethane

The apparatus used for preparation of azomethane is shown in Figure 1a. The method we used is a slightly modified version of the Renaud and Leitch preparation procedure.

Ten grams of Sym-1,2-dimethylhydrazinedihydrochloride (obtained from Aldrich Chemical Co.) was slowly added to 25 ml of 6N NaOH contained in a 250 ml Erlenmeyer flask. The flask was cooled in an ice bath and the contents vigorously stirred using a magnetic stirrer. When 10 gm of Sym 1,2-dimethylhydrazinedihydrochloride was added, ∿ 3 ml of 6N NaOH was mixed with this solution to dissolve any remaining solid. This solution was transferred to the dropping funnel.

35 grams of mercury (II) oxide was mixed with 50 ml of distilled water in the three-necked 500 ml flat-bottom flask. The three-necked flask was connected on one side to a helium tank and another side to a cold finger. The cold finger, maintained at 0°C with crushed ice, was connected to two glass traps in series. Both traps were cleaned by flaming them under vacuum.

Before starting the addition of the solution present in the dropping funnel to the three-necked flask, the assembled system was flushed with He for at least one hour to remove all traces of air present in the assembly. The first trap was maintained at 193K (dry ice-trichloroethylene slush) and the second at ∿ 163K (ethanol cooled with liquid N_2). The solution in the dropping funnel was added in drops to the slurry of mercuric oxide which was slowly stirred with a magnetic stirrer. The addition was completed in ∿ 45 minutes and He allowed to flow for another

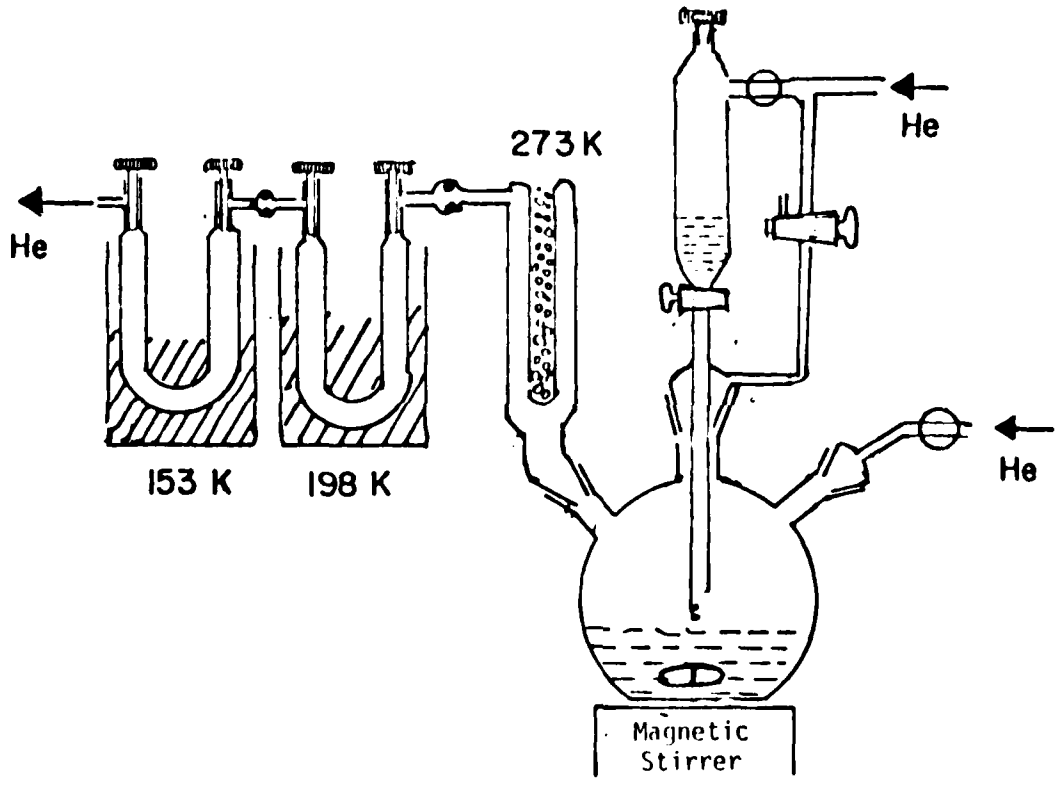

Figure 1a. Apparatus for the Preparation of Azomethane.

20 minutes to sweep out any remaining azomethane in to the traps. (The flow rate of helium was ∿ 20 ml/min.)

The traps were disconnected from the assembly and cooled to 77k with liquid N_2 to pump out He before transferring the contents to a bulb. The cold finger of the bulb was then maintained at 197K and azomethane distilled into a storage vessel maintained at 77K. The first and the last fractions were discarded. The vapor pressure of azomethane at 197K is ∿ 7 torr while that of H_2O is less than 1×10^{-3} torr which enabled us to separate the two.

All preparation and handling of azomethane was carriec out in the dark or under red lights to avoid photolysis. The azomethane was stored at 197K.

APPENDIX II

Generation of the 257 nm CW UV Laser Beam

A schematic diagram of the setup is shown in Figure 2a. A Lexel model 95 Argon ion laser was operated on the 514 nm line. The out of this laser was checked to ensure that the laser was operating in TEM_{oo} mode. The Gaussian beam was focused using a 10 cm focal length quartz plano convex lens to obtain a tight beam waist with a confocal parameter of 10 cm. (The focal length at 514 nm of the lens was accurately measured using the cat's eye technique) The position of the lens was adjusted to locate the beam waist in the middle of a 50 mm long (10 mm x 10 mm on the side) ADP crystal (Inrad Corp.) which was housed in a gold plated copper block. This copper block was in snug contact with a gold plated pedestal which was backed by a Paltier thermoelectric cooler. The Peltier cooler itself was backed by a heater block which, in turn, was cooled by circulating water at a constant temperature ($\pm$ 2 °C) from a temperature controlled five gallon water bath heated by a fish tank heater. By adjusting the rate of water flow and the temperature of the heater block (which was controlled by a proportional heater) the temperature of the ADP crystal could be maintained at -10 °C with a precision of $\pm$ 0.1 °C. We found that the doubled 257 nm output was a maximum at this temperature.

The 257 nm beam was diverging as it exited the crystal; this beam was rendered parallel by a second lens ($\sim$ 15 cm focal length at 257 nm). The collinear 257 nm and 514 nm beams were dispersed by a prism and the 514 nm beam stopped by a block. The entire assembly was housed inside a box to prevent dust from getting in and 514 nm light from scattering out.

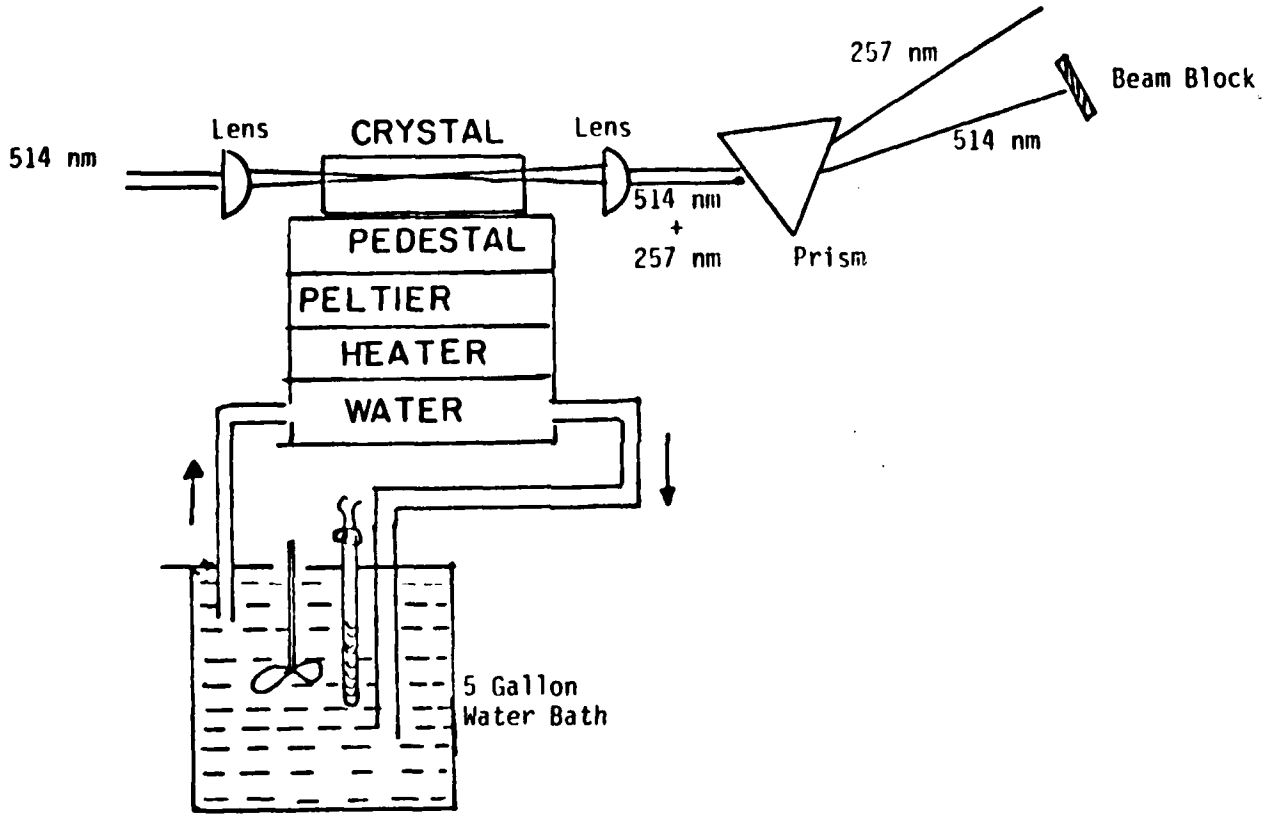

Figure 2a. Details of the Second Harmonic Generation Set Up.

With an input energy of 1 W at 514 nm, we could routinely obtain $\sim 50\mu W$ of 257 nm, which was more than adequate to carry out our experiments.

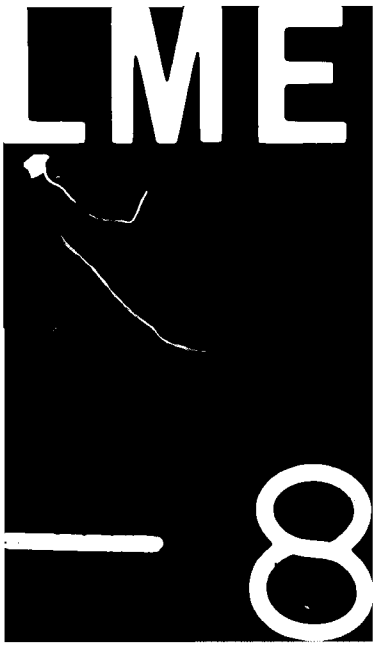
LME
8